Accepted Manuscript

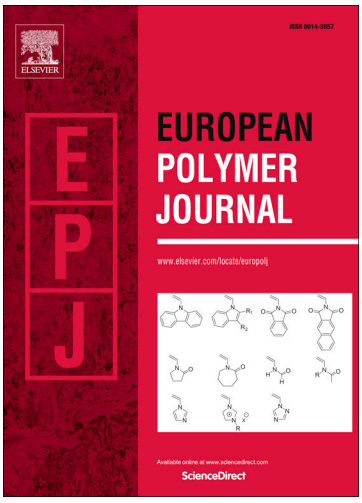

Luminescent SiO_2 nanoparticles for cell labeling: combined water dispersion polymerization and 3D condensation controlled by oligoperoxide surfactant-initiator.

Catherine Cropper, Nataliya Mitina, Olga Klyuchivska, Khrystyna Harhay, Rostyslav Stoika, Valentina Glazunova, Zoryana Nadashkevich, Orest Hevus, Yaroslav Z. Khimyak, Alexander Zaichenko

PII: S0014-3057(18)30030-2
DOI: https://doi.org/10.1016/j.eurpolymj.2018.04.008
Reference: EPJ 8364

To appear in: *European Polymer Journal*

Received Date: 5 January 2018
Revised Date: 5 April 2018
Accepted Date: 9 April 2018

Please cite this article as: Cropper, C., Mitina, N., Klyuchivska, O., Harhay, K., Stoika, R., Glazunova, V., Nadashkevich, Z., Hevus, O., Khimyak, Y.Z., Zaichenko, A., Luminescent SiO_2 nanoparticles for cell labeling: combined water dispersion polymerization and 3D condensation controlled by oligoperoxide surfactant-initiator., *European Polymer Journal* (2018), doi: https://doi.org/10.1016/j.eurpolymj.2018.04.008

Luminescent SiO_2 nanoparticles for cell labeling: combined water dispersion polymerization and 3D condensation controlled by oligoperoxide surfactant-initiator.

Catherine Cropper[a], Nataliya Mitina[b], Olga Klyuchivska[c], Khrystyna Harhay[b], Rostyslav Stoika[c], Valentina Glazunova[d], Zoryana Nadashkevich[b], Orest Hevus[b], Yaroslav Z. Khimyak[a,e]*, Alexander Zaichenko[b*]

[a]University of Liverpool, Department of Chemistry, Crown Street, L69 7ZD, Liverpool, United Kingdom
[b]Lviv National Polytechnic University, Institute of Chemistry, Department of Organic Chemistry, Lviv 79013, Ukraine.
[c]Institute of Cell Biology of NAS of Ukraine, Department of Regulation of Cell Proliferation and Apoptosis, 79005, Lviv, Ukraine.
[d]O.O. Galkin Institute of Physics and Engineering of NAS of Ukraine, Department of Physical Materials Donetsk, Ukraine
[e]School of Pharmacy, University of East Anglia. Norwich Research Park, Norwich, 7TJ United Kingdom.

Keywords: functional oligoperoxide, graft-polymerization, siliceous nanoparticles, particle morphology, rhodamine encapsulation, cell labeling, solid state NMR

ABSTRACT: Hybrid polymer coated silica nanoparticles (NPs) were synthesized using low temperature graft (co)polymerization of trimethoxysilane propyl methacrylate (MPTS) initiated by surface-active oligoperoxide metal complex (OMC) in aqueous media. These NPs were characterized by means of kinetic, solid-state NMR, TEM and FTIR techniques. Two processes, namely the radical graft-copolymerization due to presence of double bonds and 3D polycondensation provided by the intra- or/and intermolecular interaction of organosilicic fragments, occurred simultaneously. The relative contribution of the reactions depending on initiator concentration and pH value leading to the formation of low cured polydisperse microparticles or OMC coated SiO_2 NPs of controlled curing degree was studied. The availability of free-radical forming peroxide fragments on the surface of SiO_2 NPs provides an opportunity for seeded polymerization leading to the formation of the functional polymer coated NPs with controlled particle structure, size, and functionality. Encapsulation of the luminescent dye (Rhodamine 6G) in SiO_2 core of functionalized NPs provided a noticeable increase in their resistance to photo-bleaching and improved biocompatibility. These luminescent NPs were not only attached to murine leukemia L1210 cells but also tolerated by the mammalian cells. Their potential use for labeling of the mammalian cells is considered.

TOC graphic:

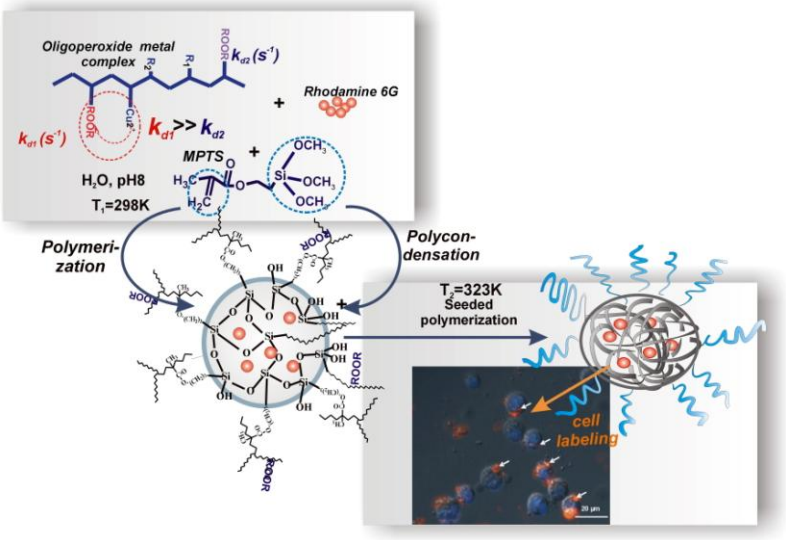

* Corresponding authors. Alexander Zaichenko (zaichenk@lp.edu.ua), Yaroslav Z. Khimyak (y.khimyak@uea.ac.uk)

1. Introduction

The biocompatible NPs with cured SiO_2 core and specific organic fragments on their surface are of great interest for providing tailored functionality. They might be used as analytical reagents in diagnostics, including the magneto-sensitive and luminescent labeling of the pathological cells *in vitro* and the MRI labels *in vivo*, as well as carriers for targeted drug delivery [1-8].

There are numerous approaches for synthesis of the organosilica nanocomposites for the biomedical applications [9-15]. Almost all of them are based on the sorption functionalization of fumed or porous silica colloid precursors and subsequent reactions of functional fragments immobilized on their surface [10, 14, 16, 17]. The organosilicic methacrylate (MPTS) and derived copolymers are widely used for surface functionalization of both inorganic [18] and polymeric [19] particles. MPTS is a bifunctional monomer that is used as a curing agent for obtaining hydrogels including materials for dental applications [20, 21]. The hydrolysis of its organosilicic fragments was studied in [22, 23]; it occurs slowly at 323-343K and is accelerated in the acidic medium [20, 24]. However, some researchers confirmed independence of the hydrolysis rate on the pH value [21, 25].

It was shown that mesoporous functional SiO_2 particles can be synthesized in two-stage process, first via obtaining SiO_2 particles and then through modification of their surface [26, 27]. Besides, sol-gel method of synthesis in the mixture of TEOS and MPTS can be used [28, 29]. The availability of unsaturated fragment on the particle surface provides a possibility for their further modification [30]. Thereisa limited number of publications [31, 32] concerning a simultaneous controlled synthesis and functionalization of SiO_2 NPs *in situ*. Synthesis of hybrid polymer/inorganic particles via water dispersion multi-stage polymerization was described [33]. First polystyrene particles were obtained by means of water dispersion polymerization till 80% of monomer conversion, then MPTS was added to the system containing polymer-monomer particles and polymerization was continued. A possibility of controlling the reaction of formation -O-Si-O-Si- bonds changing pH value was ascertained [33]. It was found [22] that compactly packed SiO_2 nanoparticles can be obtained by hydrolytic condensation of the organosilicic fragments of MPTS molecules in the acidic medium. The final products here are intramolecular circles consisting of 6-24 atoms of Si till 1,500 g/mole molecular weight silsesquioxanes or poly(silsesquioxanes). The investigators also noticed that a simultaneous copolymerization prevents the reaction of the organosilicic fragments and formation of SiO_2 particles. Polymerization of MPTS leads to a formation of cured structures of uncontrolled size and shape. At the same time, MPTS and polymers containing MPTS links and blocks can be used for controlled synthesis of cured SiO_2 particles in mixtures with the tetraethoxysilane (TEOS) [34]. As a result of MPTS interaction with TEOS, they form cured particles containing the unsaturated double bonds of MPTS on the surface [22]. The preparation of the linear poly(MPTS) and block-copolymers poly(MPTS)-block-poly(MMA) that were further used for obtaining cured and star-like polymers was described [35]. Porous coatings were obtained using block-copolymers poly(styrene)-block-poly(MPTS), as shown in [36]. As a result of MPTS radical

polymerization initiated by the AIBN, poly(MPTS) was synthesized, then cured polymer was obtained in water-alkaline solution in the presence of acid as a promoter of the polycondensation [37]. However, the researchers could not obtain cured SiO_2 nanoparticles when using that approach. The proposed scheme suggests that condensation occurs between MPTS fragments in the polymer molecules and free MPTS. For obtaining of SiO_2 nanoparticles, two-stage process was proposed: first, MPTS block-copolymers containing hydrophilic blocks were synthesized, then particles consisting of SiO_2 core and stabilizing the hydrophilic blocks were obtained by sedimentation of the polymers in water [38, 39]. SiO_2 particles of the "core-shell" structures were obtained using seeded water dispersion polymerization of MPTS in the presence of the polystyrene particles [19, 40, 41, 42]. Water dispersions of the nanoparticles consisting of SiO_2 core were obtained via subsequent polymerization stages [43]: a silicic acid and MPTS were added to water for obtaining seeds, then other monomers were provided to carry out an initiated radical copolymerization. It was shown [44] that the increase of MPTS concentration to 4% in the monomer mixture leads to a formation of the unstable dispersions. However, even very small amount of the monomer organosilicic fragments provides obtaining of the polymers forming durable hydrophobic films from water dispersions. In order to avoid the uncontrolled hydrolysis and intermolecular cross-linking during MPTS polymerization [45, 46], the synthesis of MPTS containing functional copolymers via copolymerization with surface-active monomers in the organic solution was proposed with a subsequent dispersion in water in the presence of catalyst that accelerates the hydrolysis of the organosilicic groups. The influence of concentration and nature of the radical initiators on the behavior of these reactions has not been studied yet.

Conventional emulsifiers and initiators for MPTS water dispersion polymerization do not yield spherical SiO_2 nanoparticles and their stable dispersions. The key problem for purposeful synthesis and tailoring structures of the cured functional SiO_2 nanoparticles is a controlling of two reactions, radical polymerization and polycondensation that take place simultaneously due to the availability of the unsaturated bond and the organosilicic fragments in the MPTS molecules. A contribution of these reactions that determine the structure of cured SiO_2 core and functional shell has not been sufficiently studied. The kinetic peculiarities of these reactions and their contributions in total rate of the formation of functional SiO_2 nanoparticles in a result of MPTS radical polymerization can be a convenient tool for the predicted and controlled synthesis of the cured polymer coated SiO_2 nanoparticles.

Earlier, we have demonstrated several perspectives of the controlled synthesis and simultaneous surface functionalization of the polymeric and inorganic colloids and NPs that were successfully tested as magnetic and luminescent biomedical reagents using oligoperoxide-surfactants as radical surface-active multi-site initiators or templates and surface modifiers [47-51]. We have also studied the nucleation of the polymeric nanoparticles resulted in low-temperature water dispersion polymerization initiated by the surface-active multi-site initiator OMC [52].

Here we present the results of the kinetic and structural studies of synthesis of novel functional polymer coated SiO_2 NPs via low temperature water dispersion polymerization of MPTS initiated by surface-active oligoperoxide metal complex, as well as their application for encapsulation of the luminescent dye that can be used for labeling of the mammalian cells.

2. Experimental

2.1. Materials.

For synthesizing SiO_2 NPs coated with functional oligoperoxide, 3-(trimethoxysilyl) propyl methacrylate (MPTS) (98% purity, Aldrich) were used. Other monomers were as follows. Vinyl acetate (VA) (Labscan, Poland) was purified by vacuum distillation and its physic-chemical properties were in accordance with the literature data [53]. Maleic anhydride (MA) (Merck) was purified by vacuum sublimation, its melting point after purification was 325 K (literature data: 325.9 K [54]). The peroxide monomer 2-*tert*-butylperoxy-2-methyl-5-hexene-3-yne (CH_2=CH–C≡C–$C(CH_3)_2$–O–O–$C(CH_3)_3$)(VEP) was synthesized from the 2-methylhex-5-en-3-yn-2-ol (CH_2=CH–C≡C–$C(CH_3)_2$–OH; Nairit Plant CJSC, Armenia) and *tert*-butyl hydroperoxide(AkzoNobel, Netherlands) was purified by vacuum distillation and characterized by: [O]=8.7%, d_4^{20}=0.867 g/ml, n_d^{20}=1.4482[55]. Styrene (St) (Aldrich) and N-vinyl pyrrolidone (NVP) (Aldrich) were purified by vacuum distillation. Ammonium persulfate (PA) (Aldrich) and Azobisisobutyronitrile (AIBN) (Merck) were used as initiators after purification by recrystallization from ethyl alcohol. The emulsifier for water-dispersion polymerization - Sodium 1-pentadecanesulfonate (PSNa) (ABCR GmbH)Luminescent dye [9-(2-carboxyphenyl)-6-diethylamino-3-xantenelydene]-diethylammonia chloride (Rhodamine 6G, emission 560 nm) - was purchased from Aldrich and used without additional purification.

2.2. Synthesis

2.2.1. Synthesis of functional oligoperoxide and oligoperoxide metal complex.

Water soluble surface-active oligoperoxide metal complex (OMC) applied as a multi-site initiator was synthesized in our lab via previously reported technique [56]. General structure of OMC used as macro initiator and stabilizer at water-dispersion polymerization:

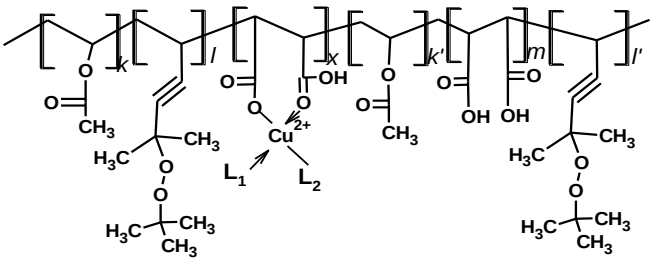

where: $k+k'$=22%; $l+l'$=34%; m=42%, x=2%, M_n~2,000 g/mol, [Cu^{2+}]=1.1%, L_1,L_2– low molecular weight ligands, for example, water molecule or alcohol.

Preparation of functional oligoperoxide (FO) poly(VA-*co*-VEP-*co*-MA) was carried out, as described in [57]. Vinyl acetate (VA, 1.53ml, 0.018mol), 2-*tert*-butylperoxy-2-methyl-5-hexene-3-yne (VEP, 3.48 ml, 0.019 mol) and maleic anhydride (MA, 1.63 g, 0.017 mol) (Aldrich) were dissolved in ethyl acetate (6.0 ml) and azobisisobutyronitrile (AIBN, 0.153g, 0.01 mol) (Merck) was added as radical initiator. Polymerization was carried out at 343 K under argon atmosphere until a monomer conversion of 65% was achieved. The resulting solution was concentrated and purified from the residual monomers by triple precipitation into hexane. The obtained copolymer was dried in vacuum until a constant weight. After 48 h, the yield was 4.0 g and copolymer was of the following composition: [VA-links]=22.8% mol, [VEP-links]=32.2%mol, [MA-links]=45.0%mol; M_n~2,000 g/mol.

The synthesis of OMC containing Cu^{2+}cations was based on using FO as a ligand. It was carried out as follows: 2 g (0.001 mol) of the FO was dissolved in 20 ml of ethanol, 0,86 g (0.005 mol) of the salt $CuCl_2$ was dissolved in 10 ml of ethanol, were added into a three-necked flask under stirring. After stirring for 0.5 h at 298 K the reaction mixture was precipitated into distilled water. OMC was carefully washed from salt with water and dried under vacuum. The content of metal cations was determined by using elemental analysis and controlled by means of atom-adsorption spectroscopy.

2.2.2. Water dispersion polymerization and copolymerization of MPTS.

Water dispersion polymerization was carried out in the dismountable dilatometers or in glass reactor equipped with a stirrer and backflow condenser. Thoroughly deoxygenated distilled water was used for dispersion polymerization under permanent argon flow, 25 % NH_4OH was used for controlling the pH value. OMC (or PA) was dissolved in water, and AIBN was dissolved in the monomer. Then monomers were added and stirred till the emulsion was formed. When OMC was used as an initiator, the polymerization was carried out at 298 K. The compositions of the systems and procedures used for water dispersion polymerization are presented in the Table 1.

Table 1. Composition of MPTS based monomer systems at water dispersion polymerization (Initiator – OMC; [monomers] per water 10%; pH=8.5; 298K)

Monomers, % mol			Content of oligomer initiator OMC	
MPTS	St	NVP	[OMC] per water phase, %	[VEP links] per monomer, mol·l^{-1}
100	-	-	0.5	0.09
100	-	-	3.0	0.54
80	20	-	0.5	0.09
80	-	20	0.5	0.09
60	-	40	0.5	0.09

2.2.3. Synthesis of Rhodamine encapsulated SiO_2 nanoparticles.

The Rhodamine encapsulated organosilicic NPs were synthesized as follows: firstly, the dye was dissolved in MPTS or in the mixture of MPTS with other monomers, OMC was dissolved in 1.25 % solution of water ammonia and pH was adjusted to pH=8 by dropping of 5 % NH_4OH. Then dye solution in monomers and aqueous ammonia solution of OMC were charged into reactor under stirring, the reaction system was purged by Ar and stirred at 298 K. Resulting NPs were purified by dialysis.

Oligoperoxide coated NPs were used for grafting functional polymeric chains via seeded polymerization initiated from their surface. Water based dispersions of the NPs and monomers were charged into glass reactor equipped with stirrer and backflow condenser and stirred at 323K.

For further characterization, the resulting NPs were separated from aqueous phase by centrifugation and re-suspending in ethanol, followed by vacuum drying. As a result, highly stable colloidal systems of polymeric NPs with functional oligoperoxide shell and controlled particle size distribution were synthesized.

2.3. Kinetic studies

2.3.1. The kinetic study of the formation of poly (MPTS) particles.

Monomer conversion was calculated via dilatometric study using the equation [58]:

$$S=(\Delta V/(V\cdot K))\cdot 100\% \quad (1)$$

V is the volume of the initial monomer (ml), ΔV is the change of the monomer volume as a result of polymerization for definite time period (ml), K is a coefficient of the contraction dependent on the monomer and polymer specific densities according with the equation:

$$K=(d_p-d_m)/d_p \quad (2)$$

d_m and d_p are specific densities of monomer and polymer, respectively ($g\cdot ml^{-1}$). Monomer conversion was determined also via gravimetric study using the equation:

$$S=(w_{SR}/[M])\cdot 100\% \quad (3)$$

where: w_{SR} is the solid residue (weight content of the polymer determined gravimetrically) of the reaction monomer-polymer mixture after the definite period of time (% w), $[M]$ is the monomer content in the initial reaction mixture (% w).

2.3.2. Estimation of specific density of SiO_2 NPs.

The specific densities of NPs were calculated taking into account comparison of dilatometric and gravimetric studies of MPTS conversion at polymerization. Substitution of the value $(\Delta V/V)\cdot 100$ % measured from dilatometric study and the value of monomer conversion determined from gravimetric study into equation (1) provides the estimation of the coefficient of contraction:

$$K=(\Delta V\cdot 100)/(S\cdot V) \quad (4)$$

Therefore, a specific density of the NPs can be calculated using the equation (2):

$$d_p=d_m/(1-K), \quad (5)$$

where: d_m for MPTS is equal to 1.045 $g\cdot ml^{-1}$.

2.3.3. Calculation of the particle formation rate.

The overall rate of SiO_2 particle formation at MPTS polymerization$R_{p+pc}$$mol\cdot(l\cdot s)^{-1}$consisting of the rates of radical polymerization (R_p) and formation of cured core in a result of reaction polycondensation

of MPTS organosilicic fragments (R_{pc}) was determined on stationary section of kinetic curve of total change of monomer conversion on time [59] in coordinates S – τ.

In order to suppress the radical polymerization with participation of MPTS double bond stable radical 2,2-Diphenyl-1-picrylhydrazyl (DPPH) (Aldrich) (0.03–0.15 mmol·l^{-1}in MPTS) was used and induction period (τ_{ind}) was determined. Constant value of the ratio $[DPPH]/\tau_{ind}$at different concentrations of inhibitor witnesses that all growing radicals interact with inhibitor molecules and chain termination as a result of growing radical interaction doesnot occur [58]. This allows determining a separate rate of SiO_2 particle formation due to the polycondensation reaction only from the kinetic curves obtained in the presence of inhibitor in the reaction mixture.

2.4. Characterization

2.4.1. Measurement of particle size.

The NPs size in water dispersions was measured by a transmission electron microscope JEM-200A (JEOL, Japan) at an accelerating voltage of 200 kV. The samples of the water dispersion of the NPs were diluted with distilled water to a concentration of 0.1g/100ml NPs (solid residue) and pH 7.2–7.8. Samples were prepared [60] using the method of spraying the tested solution on a substrate by means of the ultrasonic dispersant UZDN-1A (UkrRosPribor Ltd, Ukraine), which allows obtaining a uniform coating substrates. A thin amorphous carbon film deposited on a copper grid was used as a substrate. Dispersant options: type UZDN-1 possessing power of 50W and frequency of 35 kHz. Hydrodynamic diameter of the particles were measured by a dynamic light scattering technique (DLS) with Zetasizer Nano ZS (Malvern Instruments GmbH, Stuttgart, Germany) instruments and by photon correlation spectroscopy using the Non-Invasive Back Scatter technology (NIBS) at 298 K. The samples for DLS measurements were prepared by a diluted water dispersion of the NPs with distilled water to a concentration of 0.04g/100ml NPs (solid residue) and pH 7.2–7.8.

2.4.2. NMR spectroscopy.

All solid-state NMR experiments were conducted at 9.4 T using a Bruker DSX-400 (Bruker, Germany) spectrometer operating at 79.49, 100.61 and 400.13 MHz for ^{29}Si, ^{13}C and ^{1}H respectively. All chemical shifts are quoted in ppm from external TMS. ^{1}H-^{13}C CP/MAS NMR spectra were acquired at an MAS rate of 10 kHz. A ^{1}H π/2 pulse length was 3.0 μs and the recycle delay was 8.0 s. The CP contact time was 1.0 ms with the Hartmann-Hahn matching condition set using Hexamethyl benzene (HMB). ^{1}H-^{29}Si CP/MAS NMR spectra were acquired at an MAS rate of 4.0 kHz. A ^{1}H π/2 pulse length of 3.1 μs and the recycle delay of 10 s were used during acquisition. The CP contact time was 2.0 ms with the Hartmann-Hahn matching condition set using kaolinite.

2.4.3. Luminescent spectroscopy.

Luminescence measurements were performed using laboratory spectral complex based on the MDR-2 and MDR-12 monochromators (LOMO, Russian Federation). The Deuterium LDD-400 was used as light source for luminescence excitation. The luminescence was excited by the monochromatized light using the primary MDR-2 monochromator. The luminescence was analyzed using the MDR-12 monochromator. The PMT FEU-100 was used for light intensity registration.

2.5. Cell culture experiments

Murine lymphocytic leukemia cells of L1210 line were obtained from the Institute of Experimental Pathology, Oncology and Radiobiology of National Academy of Sciences of Ukraine (Kyiv, Ukraine). Cells were cultured in the DMEM medium (Sigma, sake) supplemented with 10 % fetal bovine serum (FBS; Sigma). For experiments, cells were grown in plastic culture flasks that were kept in the thermostat under 5 % CO_2atmospheres at 310K and 100 % humidity.

A suspension of the Rhodamine containing NPs was added to final concentration of 0.6 $mg \cdot ml^{-1}$ (dilution 1:200, initial concentration of NPs in the dispersion equaled 12 %) in the DMEM medium in which L1210 cells were cultured for 24 h [61]. Cell viability was monitored by using the Trypan blue exclusion test that is based on staining of dye-permeable dead cells with 0.1 % Trypan blue, while the alive cells stay un-stained. Light/DIC and fluorescence microscopy of cells was conducted after their staining with Hoechst 33342 under a Carl Zeiss AxioImager A1 microscope (Carl Zeiss, Germany). Final concentration of the fluorescent dye was 0.3 $\mu g \cdot ml^{-1}$, and the staining time was 15 min. When Hoechst 33342 was used, the excitation and emission wavelengths were 365–395 nm and 445–450 nm, respectively, with blue filter, while for Rhodamine 6G staining, the excitation and emission wavelengths were 546–560 nm and 575–640 nm, respectively, with red filter. Cultured cells were photographed under a Zeiss MRm microscope with cooled digital CCD camera at constant exposure.

3. Results and discussion

In this paper, we present the results of experimental study of synthesis of polymer coated luminescent SiO_2 NPs via step-by-step polymerization initiated by multi-site OMC macroinitiator containing peroxide moieties of different thermal stability. The characteristic feature of OMC is an ability to generate free radicals including macroradicals in a wide temperature range (<298 – 353K) due to polarizing influence of the media or activating effect of coordinated metal cations on decomposition of the part of side ditertiary peroxide fragments. The decomposition of activated peroxide groups at 298K ($k_{d1(298K)}=2.5 \cdot 10^{-5}\ s^{-1}$) provides water dispersion polymerization and formation of OMC functionalized SiO_2 nanoparticles and decomposition of peroxide groups immobilized on their surface at 353K ($k_{d2(298K)}=3.0 \cdot 10^{-8}\ s^{-1}$) leads to grafting functional polymeric chains and formation of the NPs of the "core-shell" structure [52].

3.1. Water dispersion MPTS graft-polymerization initiated by OMC.

The polymerization initiated by PA or AIBN in water solution containing emulsifier PSNa leads to a formation of low cured polydisperse colloids. This coincides with the results of the studies described earlier in [22] and can be explained by absence of water soluble surface-active fragments in formed polymer structure capable of dispersing and stabilizing cured SiO_2 molecules preventing them from aggregation and sedimentation. It was ascertained [52, 62] that initiation of water dispersion polymerization by OMC as multi-site surface-active initiator leads to a formation of the polymeric NPs containing hydrophilic OMC molecules irreversibly immobilized on the particle surface. The presence of two reactive centers in MPTS molecules suggests a possibility of two independent reaction pathways during MPTS water dispersion polymerization initiated by OMC. The first process is the radical polymerization involving double bond of the organosilicic methacrylate and providing grafting its chains to the OMC backbone. The second process is a 3D condensation of $–Si(OCH_3)_3$ fragments in a structures of polymers resulting in the formation of the SiO_2 nanoscale structures of controlled size and curing degree. The contribution of these reactions into process depends on the reaction conditions and defines the properties of final composite NPs (Figure 1).

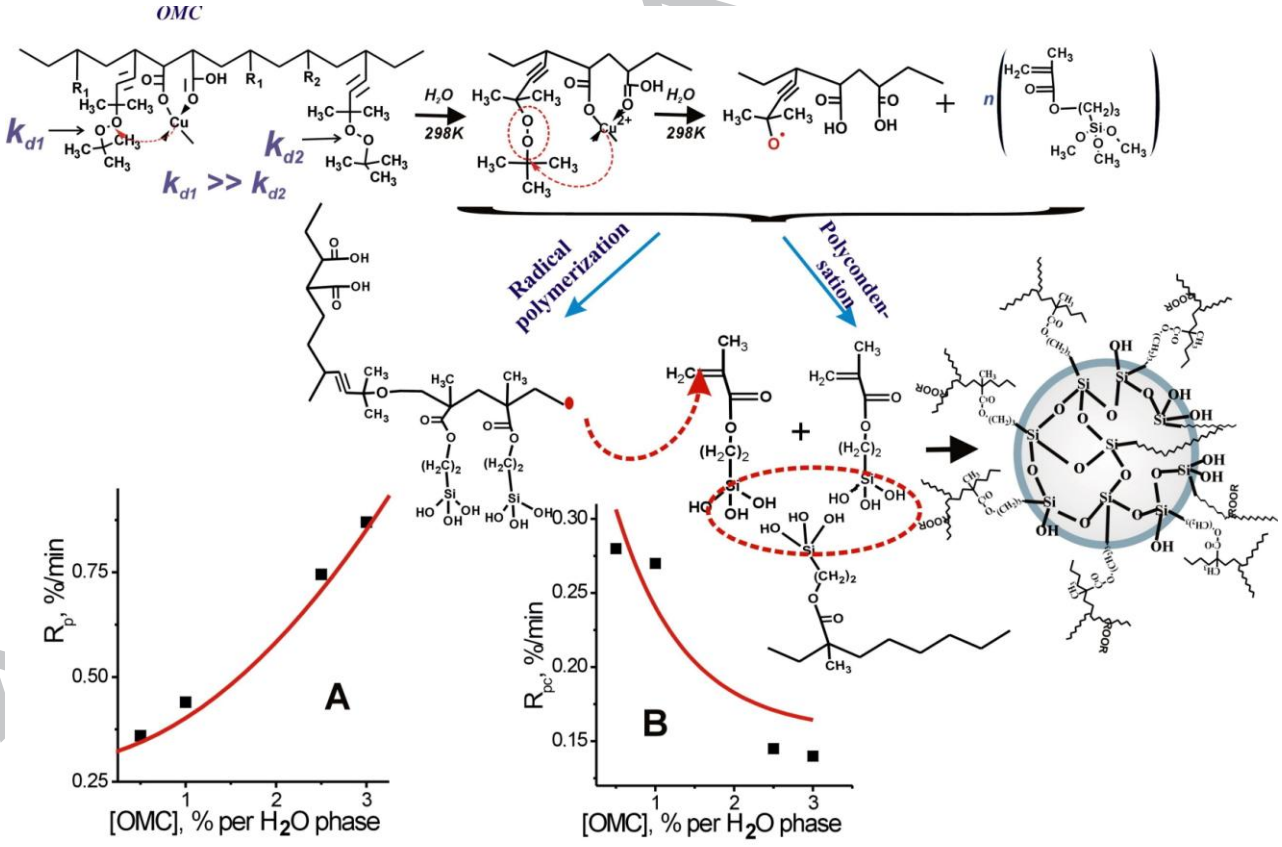

Figure 1. Scheme of the formation of OMC coated SiO_2 NPs (insets show the dependences of radical polymerization rate (A *left*)and condensation rate (B *right*) on OMC concentration.

The study of the formation kinetics, size and morphology of the NPs and local structure solid-state NMR analysis confirm the suggested scheme of the overall process of the simultaneous OMC-initiated

grafting poly(MPTS) side chains and 3D polycondensation leading to the formation of the nanocomposites consisting of cured SiO_2 core and reactive OMC shell.

3.2. Kinetic study of SiO_2 particle formation.

The kinetic curves of water dispersion polymerization of MPTS initiated by OMC (Figure 2) demonstrate that the polymerization does not follow the expected regularities of water dispersion polymerization of conventional monomers [59, 63]. If the concentration of the OMC initiator is not sufficient, the contribution of radical polymerization to the total process of NPs formation is small (polymer yield reaches 35 %) and the overall process is dominated by the 3D condensation reaction of $-Si(OCH_3)_3$ groups.

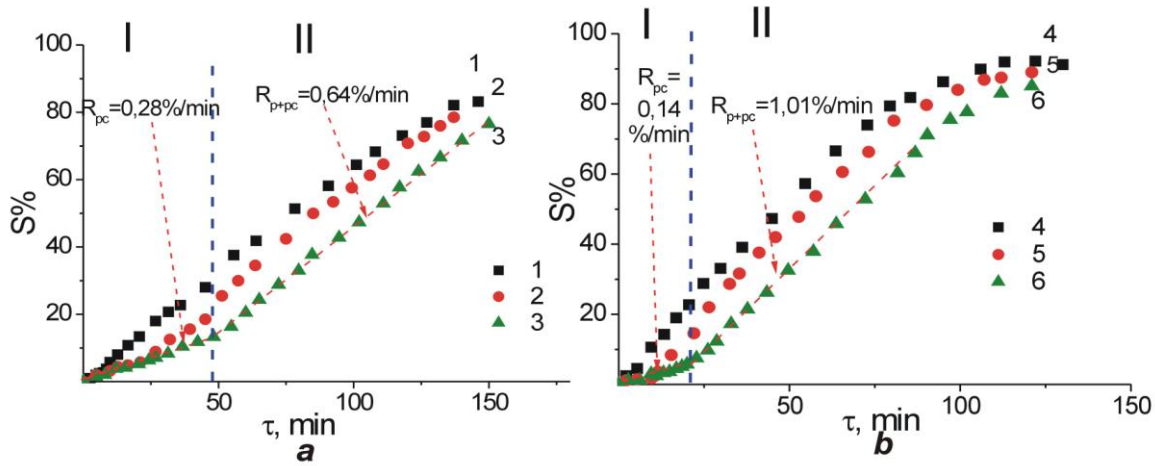

Figure2. The dependences of MPTS conversion during water dispersion polymerization on time at: [OMC]=0.5 (1-3) and 3 % (4-6) per water phase; without (1, 4) and in the presence of interceptors of free radicals [DPPH]=0.03(2); 0.06(3, 5) and 0.15(6) mmol/l per MPTS; 298K;pH=8; MPTS: H_2O ratio 1:9(section I, curves 3 and 4 polycondensation only; section II, polycondensation and radical polymerization simultaneously).

OMC coated SiO_2 NPs of a controlled size and curing degree are formed only in a result of the reaction of 3D condensation of organosilicic fragments of side poly (MPTS) chains grafted to OMC backbone. It is evident (Figure 2, the insets) that formation of solid phase in the presence of interceptor of free radicals that suppresses radical polymerization on a double bond is also observed [22]. The rate of condensation reaction and its contribution was determined from dilatometric measurements in the presence of radical interceptor when radical polymerization involving the methacrylate double bonds does not take place.

The rate of solid phase formation by MPTS depends on the amount of OMC surfactant (Figure 2). A decrease in the condensation rate when radical polymerization does not take place at the increase of OMC concentration, is caused by the lowering concentration of the molecules of MPTS participating in the reaction due to their coordination on OMC molecules, especially after a formation of the micelles at an achievement of CMC value (2% at pH 8) in the solution. After an interceptor depletion in the reaction system polymer/inorganic solid phase is formed as a result of both radical polymerization involving

MPTS double bonds and 3D condensation of $-Si(OCH_3)_3$ groups simultaneously. The conventional dependence of radical polymerization rate on OMC concentration is observed in this case (Figure 2). It is evident (Table 2) that is in contrast to dependence of the rate of condensation when radical polymerization is suppressed by presence of radical interceptor, the rate of the overall process of the formation of polymer coated SiO_2 NPs increases with an increase of the concentration of OMC as an initiator of radical polymerization.

Table 2. Kinetic characteristics of the poly (MPTS) polymerization initiated by OMC (298 K, pH=8, monomer: H_2O ratio 1:9)

[OMC], % per H_2O phase	[VEP-links] ($g \cdot mol^{-1}$)	R_{p+pc}, $(mol \cdot l^{-1} \cdot s^{-1}) \cdot 10^4$	R_{pc} $(mol \cdot l^{-1} \cdot s^{-1}) \cdot 10^4$	$R_p = R_{p+pc} - R_{pc}$ $(mol \cdot l^{-1} \cdot s^{-1}) \cdot 10^4$	R_i, $(mol \cdot l^{-1} \cdot s^{-1}) \cdot 10^7$
0.5	0.09	4.30	1.88	2.42	0.18
1.0	0.18	4.77	1.81	2.96	0.29
2.5	0.45	5.97	0.97	5.00	0.99
3.0	0.54	6.78	0.94	5.84	1.25

The higher OMC concentration results in an increased yield of the polymer up to 95%. The water dispersion polymerization initiated with 3% OMC (Figures 3, 4) leads to the formation of stable colloidal systems consisting of spherical NPs with a narrow size distribution. Such particles are protected from aggregation and sedimentation. This can be explained by the realization of both reactions i.e. radical initiated grafting and 3D condensation of MPTS chains in confined zones that are micelle-like structures formed by OMC molecules and growing polymer-monomer particles (PMP). A lower content of OMC (0.5 % in water phase) is not sufficient to promote the formation of such micelle-like structures wherein elementary stages of the radical polymerization can be realized. This causes the prevalence of the 3D condensation in comparison with radical polymerization. As a result, the particles with a wide particle size distribution (Figure 3) are formed.

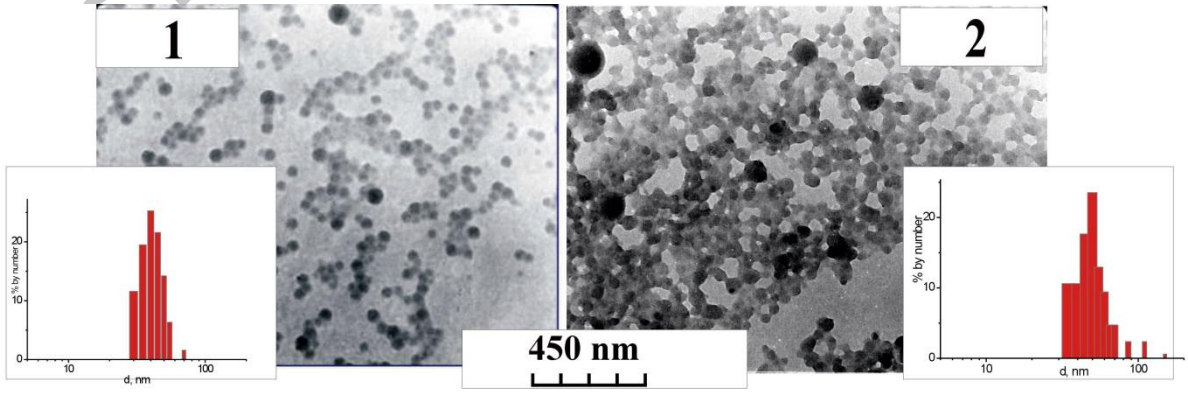

Figure 3.TEM images of the NPs obtained *via* water-dispersion polymerization initiated by 3% (1) and 0.5% (2) of OMC, pH=8(callouts are bar graphs of the particle size distribution).

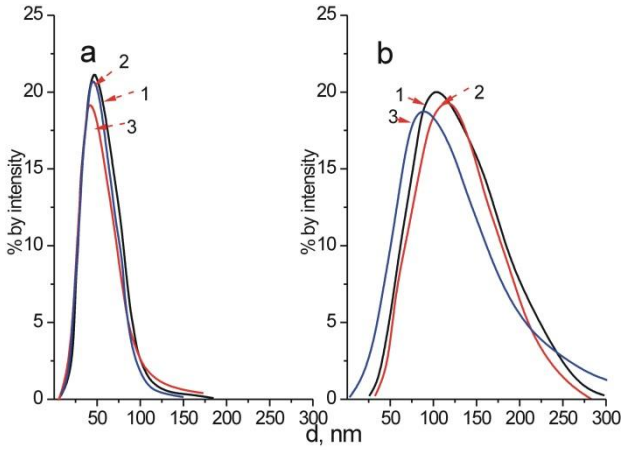

Figure 4. Curves of distribution of hydrodynamic diameters of NPs in water dispersions obtained with 3% (a) and 0.5% (b) of OMC, pH=8 (1,2,3 – measurements were recorded at 1 min intervals).

An increased contribution of radical polymerization in the total process as a result of copolymerization of MPTS with other monomers yields the NPs consisting of the grafted branches containing links of MPTS and styrene. This leads to smaller NPs with a narrowed particle size distribution (Figure 5).

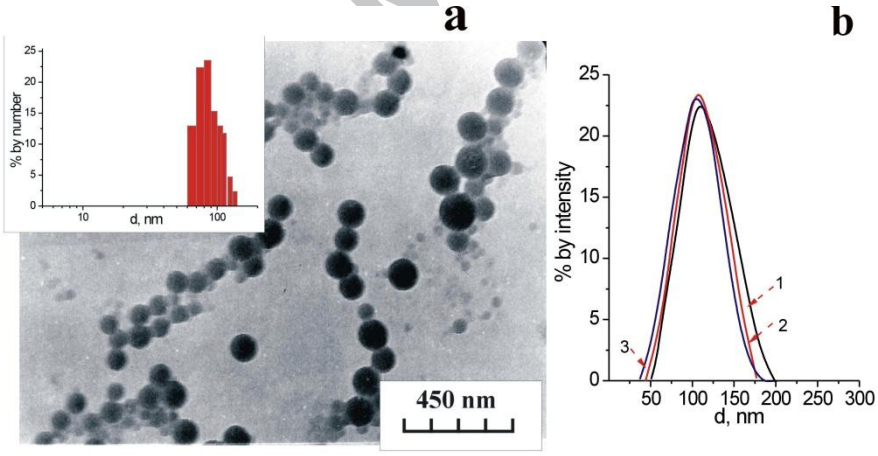

Figure 5. TEM images of the NPs of poly(MPTS-*co*-St) (callout is bar graph of the particle size distribution) (a) and distribution of NPs hydrodynamic diameters (index of polydispersity PI=0.95) (b) synthesized via water dispersion polymerization initiated by 0.5% of OMC (1, 2, 3 – measurements were recorded at 1 min intervals).

It is evident that at the enhanced OMC concentration the contribution of the rate of 3D condensation is much lower in comparison with contribution of the rate of radical polymerization in a total rate of the formation of cured SiO_2 NPs.

3.3. Interrelations between mechanisms of the formation and NPs structures.

The ^{1}H-^{13}C CP/MAS NMR spectrum (Figure 6) of the NPs formed via the radical polymerization initiated by 0.5 % of OMC shows the presence of peaks attributable to the residual unreacted double bonds (125 and 137 ppm) and carbonyl group (167 ppm) of the initial monomer. This indicates that a low

content of OMC is not sufficient for the radical grafting the MPTS chains. This is confirmed by a low intensity of the peaks corresponding to carbon sites in polymer chains (45.6 and 50.8 ppm). ^{1}H-^{29}Si CP/MAS NMR spectra also suggest the preferential formation of 3D silica network in cases when the amount of radical initiator OMC is not sufficient for graft-polymerization of MPTS. For the NPs obtained as a result of polymerization initiated by 0.5% of OMC, a higher level of silica condensation was observed. This is evident from the peak at -67.6 ppm corresponding to ^{3}T (R-Si(OSi)$_3$) sites indicative for a formation of a 3D network (Figure 7).

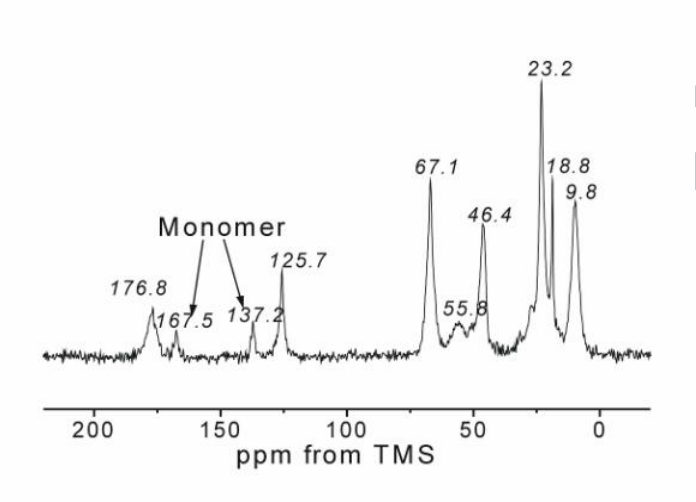

Figure 6. ^{1}H-^{13}C CP/MAS NMR spectrum of poly(MPTS) ([OMC]=0.5% per H_2O). Note that the peaks at 167.5 and 137.2 ppm are from monomer units confirming a lower level of radical polymerization.

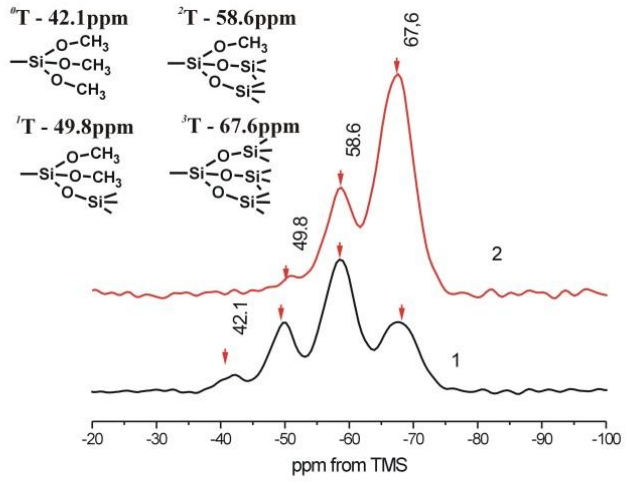

Figure 7. ^{29}Si MAS NMR spectra of (poly(MPTS), [OMC]=3.0%per H_2O (1) and [OMC]=0.5% per H_2O (2).

At the same time, the ^{29}Si NMR spectrum of SiO_2 NPs synthesized in the presence of a larger amount of OMC (Figure7) shows a higher proportion of ^{29}Si sites with a lower degree of condensation (i.e. ^{2}T at -57.6 ppm). We also observed the initial trimethoxysilyl fragments (line at -42.1 ppm) which were not involved into the condensation (Figure 7). As a result of a successful radical polymerization initiated by the larger amount of OMC, double bonds of initial monomer were not detected in the ^{13}C

solid-state NMR spectrum (Figure 8) at the expense of a significant increase of the intensity of peaks corresponding to carbon atoms of polymeric chains grafted to OMC backbone. An increased contribution of a peak at 55.8 ppm corresponding to methoxy- groups of $–Si(OCH_3)_3$ fragments in the NMR spectrum of the NPs synthesized with the larger amount of OMC confirms the predominant contribution of radical polymerization with participation of MPTS unsaturated bonds.

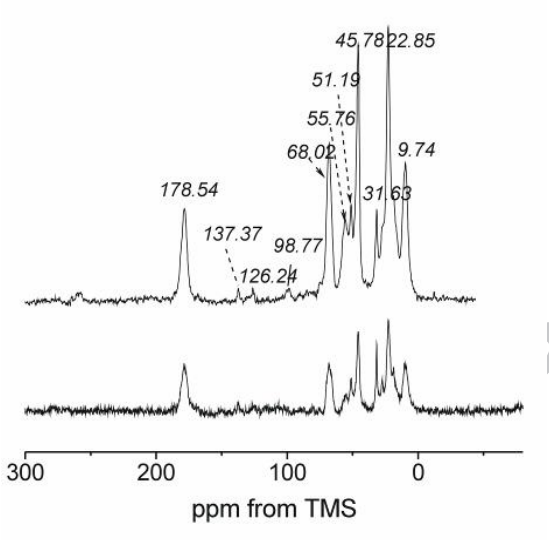

Figure 8. ^{1}H-^{13}C CP/MAS NMR (top) and $^{13}C\{^{1}H\}$ MAS NMR (bottom) spectra of poly(MPTS), [OMC]=3 % per H_2O).

An addition of other monomers *i.e.* St or NVP to the unsaturated siliceous monomer MPTS leads to an increase in the rate and the yield of the radical graft-polymerization evidenced by an intense ^{13}C peak at 50.7 ppm corresponding to carbon atoms of polymeric chains (Figure 9), even at a low content of the radical initiator OMC. However, the intensities of the peaks attributed to monomer fragments of MPTS in the NMR spectra of the product of MPTS polymerization or its copolymer with St are very similar.

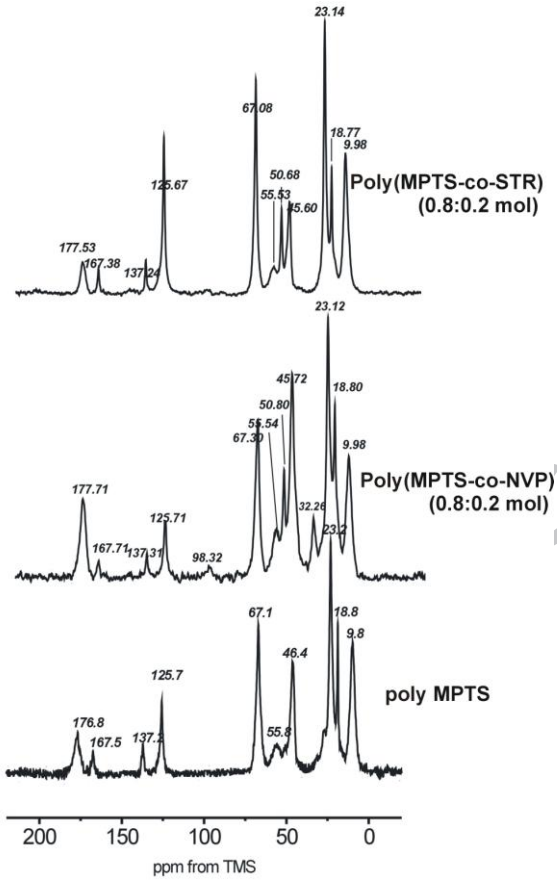

Figure 9. ^{1}H-^{13}C CP/MAS NMR spectra of the poly (MPTS) and poly (MPTS-*co*-St) and poly (MPTS-*co*-NVP).

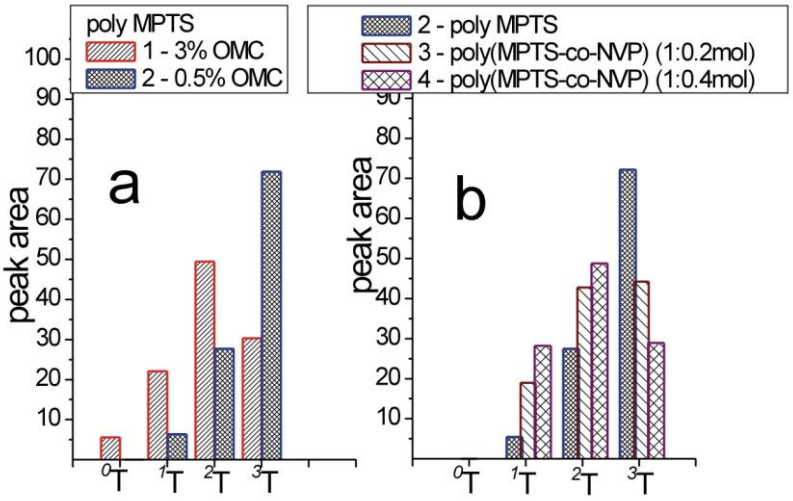

Figure 10. a) Population of ^{n}T-sites with different degree of condensation in the hybrids polyMPTS formed at concentration of OMC: 3% (1); 0.5% (2); b) changes in population of different ^{n}T-units as the result of the reactions of trimethoxysilyl fragments of NPs synthesized by polymerization of MPTS only (2) and MPTS copolymers with NVP (3, 4) initiated by 0.5% per water of OMC.

Changes in the intensity of ^{n}T-sites with different degree of condensation derived from ^{29}Si NMR spectra (Figure 10), confirm a higher degree of condensation for the products formed when the amount of radical initiator OMC was not sufficient for the radical graft polymerization.

Taking into account ^{29}Si NMR spectra (see Supplementary, Fig. S1), it is evident that the degree of condensation of the organosilica matrix in NPs formed by MPTS fragments at copolymerization with other monomers differs from that for the NPs obtained as a result of homo-polymerization of MPTS. A decreased population of ^{3}T organosilicic units was observed upon the copolymerization of MPTS with other monomers (Figure 10b; see Supplementary, Fig. S1). Moreover, this trend was further corroborated with an increased amount of additional (co)monomers in the polymerization system.

3.4. Variation in cured SiO_2 core density.

From the previous section, it can be concluded that a variation of pH and the content of surface-active macroinitiator OMC in reaction system provides control of 3D condensation reaction of trimethoxysilyl fragments of grafted side chains as well as that for the curing degree of SiO_2 core. The degree of cross-linking of the core of NPs defines the density of the inorganic core. The polymerization kinetic curves calculated from the dilatometric studies (Figure 11a, b) taking into account a contraction coefficient (e.g. change of density of the reaction system as a result of the conversion of monomers into polymers) and those obtained from the gravimetric measurements of the total yield of polymers are significantly different. This can be explained by a difference in the values of specific density of final polymer/SiO_2 NPs.

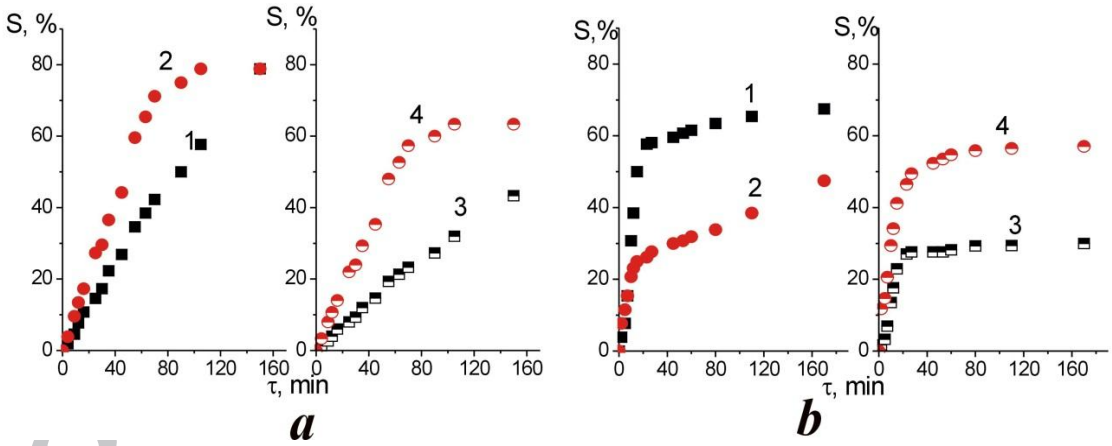

Figure 11. a) A dependency of MPTS conversion S, % (1, 2) and solid content (3, 4) in the reaction mixture characterizing the yield of MPTS water dispersion polymerization vs time at: pH=8 (a), 12 (b), [OMC]=0.5% (1, 3) and 3% (2, 4) per water phase; 298 K, monomer:$H_2$0 ratio 1:9).

A kinetic dependency of the calculated contraction coefficients confirms this assumption (Figure 12). These coefficients do not change with time as they correspond to different values of specific density of polymer composites. It is the content of OMC that determines primarily a contribution of the reactions occurring via different mechanisms. This is in a good agreement with the results of the NMR analysis discussed above. The contribution of 3D condensation, as well as the degree of the core curing, increases with a decrease in OMC concentration.

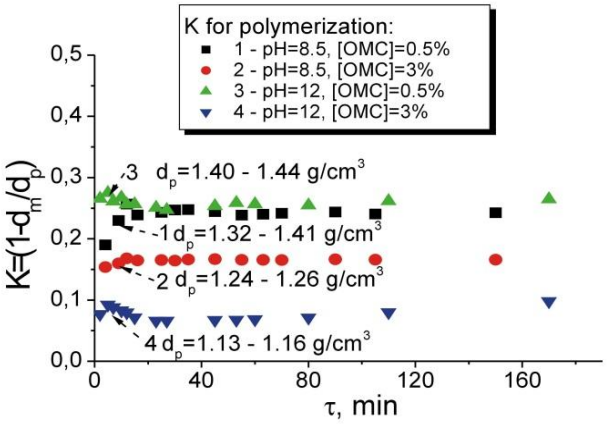

Figure 12.A dependence of the contraction coefficients on the duration of water dispersion polymerization of MPTS initiated with OMC.

Earlier, we showed [52] that only cal. 25 % of OMC di-tertiary peroxide fragments generated free radicals at room temperature due to the activating effect of the carboxyl groups and coordinated Cu^{2+}cations. Other OMC peroxide groups are more thermally stable and can enter into the structure of polymeric nanoparticles leading to the peroxide containing functional shell. Determined from experimental study coefficients of the decomposition rates for activated and non-activated peroxide groups at 298K are k_{d1}=2.5·10^{-5}c^{-1} and k_{d2}=0,003·10^{-5}c^{-1}, respectively. The peroxide groups immobilized on the particle surface are also activated as a result of a decrease of the freedom degree. This can promote the efficient initiation of the graft-radical polymerization and attachment of polymeric spacers of desired length and functionality.

3.5. Rhodamine encapsulation and formation of "core–shell" NPs via seeded polymerization.

Based on a difference in the degree of the compaction of the cross-linked SiO_2 NPs, one can assume the availability of space for the encapsulation of luminescent dye during the formation of functional NPs. The developed method of the preparation of SiO_2 NPs described in this paper, also provides the means of controlling the content of encapsulated luminescent dye in the NPs (Table 3).

Table 3. Characteristics of the NPs containing encapsulated Rhodamine 6G as a result of MPTS water dispersion polymerization (298 K, 0.4% of the dye per MPTS, H_2O: MPTS = 1:9, pH 8.5).

Concentration of OMC in water phase, %	Particle size, nm	Content of Rhodamine per NPs, %
1.0	38±9	0.35
3.0	28±6	0.26

A 2.5-fold decrease in the particle size leads to a decrease in Rhodamine content encapsulated in the core of the NPs by only cal. 30%. It is evident that the Rhodamine encapsulated SiO_2 NPs are characterized by a very narrow size distribution (PI=0.99) in the range of 28-30 nm for the main fraction (Figure13). The availability of a sufficient amount of OMC molecules on the nanoparticle surface

prevents their aggregation. In spite of a slight enlargement of the particle size (from 25–30 to 35–40 nm) after graft-polymerization, they showed a narrower particle size distribution (Figure 13).

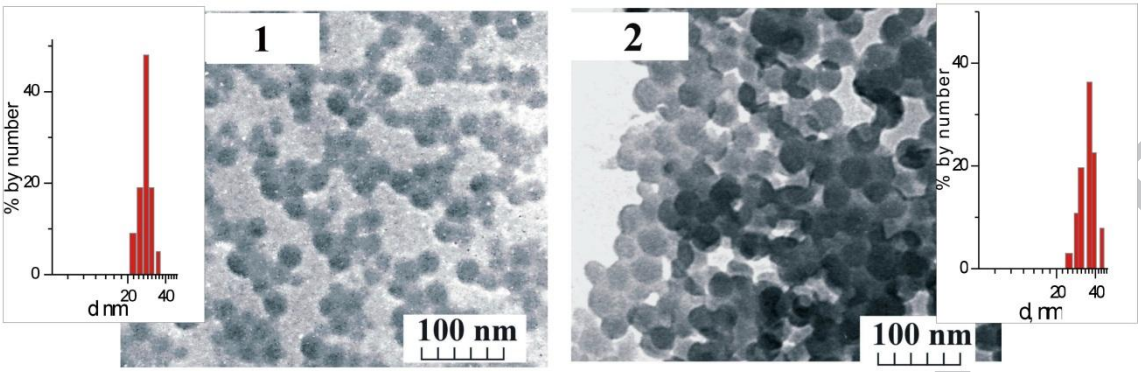

Figure 13. TEM images of the oligoperoxide coated SiO_2 NPs containing encapsulated Rhodamine (1) and NPs after the grafting polymeric chains consisting of NVP and GMA links (2) (inserts contain bar graphs of the particle size distribution).

Polymeric spacers with a tailored chain length and functionality were grafted covalently *via* polymerization initiated from the surface of oligoperoxide coated NPs. As a result of seeded polymerization, NPs containing poly(NVP) and poly(GMA) grafted chains were formed. This was confirmed by FT-IR spectra (see Supplementary, Fig. S2). The intense absorption band at 1,713 cm^{-1} observed in IR-spectrum of MPTS based OMC coated NPs corresponds to stretching vibrations of –C=O in methacrylate fragment on the particle surface. The bands at 1,380 and 1,450 cm^{-1} might be attributed to stretching vibrations of $–CH_3$ group of the methacrylate fragment. The wide intensive band at 1,000–1,150 cm^{-1} corresponds to stretching vibrations of Si–O– fragment in Si–O–Si and Si–O–C fragments. The bands at 2,900–3,000 cm^{-1} are attributed to the stretching vibrations of $–CH_2$ and –CH groups due to a formation of the polymeric chains. The appearance of the intense absorption band at 1,650 cm^{-1} corresponding to the –(O)–N– fragment of NVP in the IR spectrum of the NPs after the seeded polymerization confirms the attachment of new polymeric functional spacers.

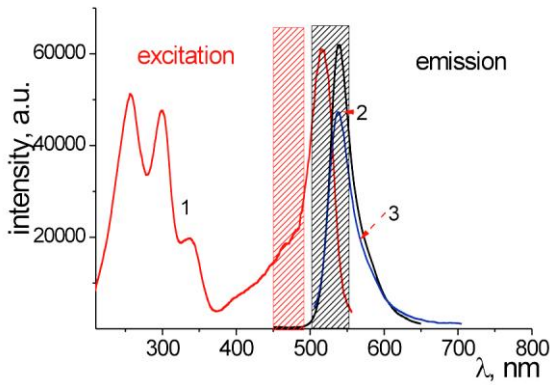

Figure 14. Spectra of excitation (1) and luminescence of water dispersions of NPs with Rhodamine 6G (2) and NPs of "core-shell" type with the grafted spacers poly(NVP-*co*-GMA) (3) (content 0.35%, λ_{ex}=320 nm, λ_{em}=540 nm).

Rhodamine-containing NPs show high luminescent ability in the same region as Rhodamine 6G and without obvious change after grafting the functional polymeric spacers (Fig. 14).

Murine leukemia L1210 cells were cultured for 24 h together with the developed NPs and stayed viable (according to Trypan blue exclusion test), thus, demonstrating their biocompatibility. As one can see from Figure 15, neither control nor the Rhodamine-encapsulated (Z3 and Z4) NPs affected growth or viability of L1210 cells after 1 day treatment of cultured cells. After 4 days of treatment with the NPs, the number of cultured L1210 cells decreased compared with the control one (without the NPs in culture medium). The less expressed increase in number of alive cells in caseswhen Z3 and Z4 NPs were used might be explained by the cytostatic rather than cytotoxic action of studied NPs, since the number of Trypan blue-positive (dead) cells did not change significantly. An attachment of these NPs to a surface of the treated cells (Fig. 16) could cause a cytostatic action (block of cell proliferation) of the NPs, although the suggested mechanism requires additional experimental approval. The applied NPs also did not affect a viability of human embryonic kidney HEK 293T cells (data not presented).

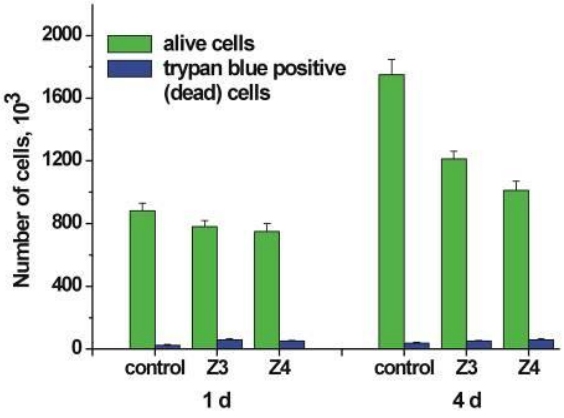

Figure 15. Results of the effect of the initial and Rhodamine-containing NPs (Z3 and Z4) on the growth and viability of murine leukemia L1210 cells (1 and 4 day cell culture).

The attachment of the developed Rhodamine-encapsulated SiO_2 NPs to cell surface (Figure 16), aswell as their resistance to rapid photo-bleaching known for other NPs labeled with specific fluorescent dyes might be two big advantages of these NPs. We found that the emission of the Rhodamine-containing NPs at 575-640 nm did not decrease significantly during 20 min UV-irradiation of L1210 cells. Since FITC-conjugated NPs were toxic for the studied cells and were bleaching even faster than Hoechst 33342 did (data not shown), we did not use them in our biological experiments.

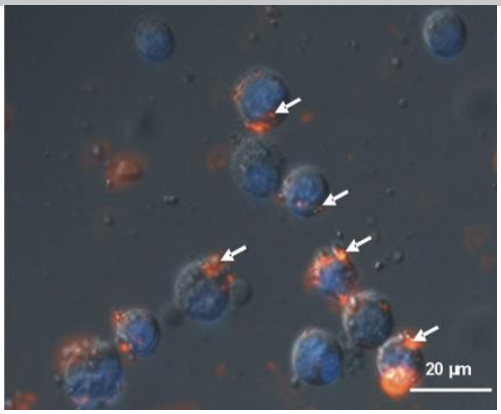

Figure 16. Murine lymphocytic leukemia L1210 cells treated for 24 h with Rhodamine G-conjugated NPs (image was obtained by a combined light and fluorescence microscopy). Micrographs of L1210 cells were taken using fluorescent microscopy after staining of cell nucleus material with Hoechst 33342 dye (blue fluorescence), while the NPs were stained in orange-red and seen attached to cell surface (white arrows).

4. Conclusions

We have developed a novel method of synthesis of functional SiO_2 NPs based on using the oligoperoxide metal complex as a low temperature surface-active multi-site initiator for water dispersion polymerization of the MPTS. It was also a convenient tool for controlling the size, density of core compaction and surface functionality of the synthesized NPs. The mechanism of the NPs formation consists of a simultaneous occurrence of 3D condensation and radical polymerization involving two MPTS reactive centers. This mechanism was confirmed by a combination of the kinetic and structural (including solid-state NMR) approaches. Fluorescent dye (Rhodamine 6G) was successfully encapsulated during the formation of the SiO_2 NPs. That provided a possibility of its further application as a fluorescent label that is well protected of the photo-bleaching and can be used for labeling the pathological mammalian cells.

Acknowledgements

The financial support of the project by the Royal Society is gratefully acknowledged. The authors express their thanks to Prof. A. Voloshinovskii and Dr. V. Vistovskiy (I. Franko National University, Lviv) for their help with interpretation of the luminescence spectrum.

Additional research data supporting this publication are available as the electronic supplementary files at the DOI: XXX.

References

[1] B.Haun, N.K.Devaraj, B.S.Marinelli, H.Lee, R.Weissleder, Probing Intracellular Biomarkers and Mediators of Cell Activation Using Nanosensors and Bioorthogonal Chemistry, ACS Nano, 5 (4), (2011) 3204–3213, http://dx.doi.org/10.1021/nn200333m

[2] Y.Zhu, Z.Li ,M.Chen, H.M.Cooper, G.Q.Lu, Z.PingXu, Synthesis of Robust Sandwich-Like SiO_2@CdTe@SiO_2 Fluorescent Nanoparticles for Cellular Imaging, Chem. Mater, 24 (3), (2012) 421-423, http://dx.doi.org/10.1021/cm2019873

[3] D.Horak, T.Shagotova, N.Mitina, M.Trchova, N.Boiko, M.Babic, R.Stoika, J.Kovarova, O.Hevus, M.Benes, O.Klyuchivska, P.Holler, A.Zaichenko, Surface-Initiated Polymerization of 2-Hydroxyethyl Methacrylate from Heterotelechelic Oligoperoxide-Coated γ-Fe_2O_3 Nanoparticles and their Engulfment by Mammalian Cells, Chem. Mater, 23 (10) (2011) 2637-2649, http://dx.doi.org/10.1021/cm2004215

[4] D.Šponarová, D.Horák, M.Trchová, P.Jendelová, V.Herynek, N.Mitina, A.Zaichenko, R.Stoika, P.Lesný, E.Syková, The Use of Oligoperoxide-Coated Magnetic Nanoparticles to Label Stem Cells, J.Biomed. Nanotechnol, 7 (3) (2011) 384-394, https://doi.org/10.1166/jbn.2011.1289.

[5] D.Tang, R.Yuan, Y.Chai, H.An, Magnetic-Core/Porous-Shell $CoFe_2O_4/SiO_2$ Composite Nanoparticles as Immobilized Affinity Supports for Clinical Immunoassays, Adv. Funct. Mater, 17(6) (2007) 976-982, https://doi.org/10.1002/adfm.200600462.

[6] L. Gai, Z. Li, Y. Hou, H.Jiang, X.Han, W.Ma, Preparation of core–shell Fe_3O_4/SiO_2 microspheres as adsorbents for purification of DNA, J. Phys. D: Appl. Phys, 43(44) (2010) 445001 (8pp), http://dx.doi.org/10.1088/0022-3727/43/44/445001.

[7] H.Wang, Y.Zhang, B.Yan, L.Liu, S.Wang, G.Shen, R.Yu, Rapid, simple, and sensitive immunoagglutination assay with SiO_2 particles and quartz crystal microbalance for quantifying *Schistosomajaponicum* antibodies, Clinical Chemist, 52(11) (2006) 2065-2071, http://dx.doi.org/10.1373/clinchem.2006.071555.

[8] S.N.Shtykov, T.Yu.Rusanova, Nanomaterials and nanotechnologies in chemical and biochemical sensors: Capabilities and applications, Russ. J. Gen. Chem, 78(12) (2008) 2521-2531, http://dx.doi.org/10.1134/S1070363208120323.

[9] M.Jaroniec, in: J.M. Loureiro, M.T. Kartel (Eds), Combined and Hybrid Adsorbents, Springer Netherlands, Amsterdam, 2006, p.23-36, http://dx.doi.org/10.1007/1-4020-5172-7_2.

[10] N.N.Khimich, Synthesis of Silica Gels and Organic-Inorganic Hybrids on Their Base, Glass PhysChem, 30(5) (2004) 430-442, http://dx.doi.org/10.1023/B:GPAC.0000045925.84139.eb.

[11] J.Go´rka, M.Jaroniec, Tailoring Adsorption and Framework Properties of Mesoporous Polymeric Composites and Carbons by Addition of Organosilanes during Soft-Templating Synthesis, J. Phys. Chem. C, 114(14) (2010) 6298-6303, http://dx.doi.org/10.1021/jp9117858.

[12] K.P.Gierszal, T.-W.Kim, R.Ryoo, M.Jaroniec, Adsorption and Structural Properties of Ordered Mesoporous Carbons Synthesized by Using Various Carbon Precursors and Ordered Siliceous P6mm and Ia3̄d Mesostructures as Templates, J. Phys. Chem. B, 109(49) (2005) 23263-23268, http://dx.doi.org/10.1021/jp054562m.

[13] Y.Cheng, R.Tan, W.Wang,Y.Guo, P.Cui, W.Song, Controllable synthesis and magnetic properties of Fe_3O_4 and $Fe_3O_4@SiO_2$ microspheres, J Mater Sci, 45(19) (2010) 5347-5352, http://dx.doi.org/10.1007/s10853-010-4583-4.

[14] A.Kierys, M.Dziadosz, J.Goworek, Polymer/silica composite of core–shell type by polymer swelling in TEOS, J. Coll. Int. Sci, 349(1) (2010) 361-365, http://dx.doi.org/10.1016/j.jcis.2010.05.049.

[15] M.Moritz, M.Łaniecki, Application of SBA-15 mesoporous material as the carrier for drug formulation systems. Papaverine hydrochloride adsorption and release study , Powder Technol, 230 (2012) 106-111, http://dx.doi.org/10.1016/j.powtec.2012.06.061.

[16] R.C.Advincula, Surface Initiated Polymerization from Nanoparticle Surfaces, J. Disper. Sci. Technol., 24 (3-4) (2003) 343-361, http://dx.doi.org/10.1081/DIS-120021794.

[17] Z.Lei, N.Ren, Y.Li, N.Li, B.Mu, Fe_3O_4/SiO_2-g-PSStNa Polymer Nanocomposite Microspheres (PNCMs) from a Surface-Initiated Atom Transfer Radical Polymerization (SI-ATRP) Approach for Pectinase Immobilization, J. Agric. Food. Chem., 57(4) (2009) 1544-1549, http://dx.doi.org/10.1021/jf802913m.

[18] B.Du, A. Mei, P.Tao, B.Zhao, Z.Cao, J.Nie, J.Xu, Z. Fan, Poly[N-isopropylacrylamide-co-3-(trimethoxysilyl)-propylmethacrylate] Coated Aqueous Dispersed Thermosensitive Fe_3O_4 Nanoparticles, J. Phys. Chem. C, 113(23) (2009) 10090–10096, http://dx.doi.org/10.1021/jp9016536.

[19] I.Tissot, J.P.Reymond, F.Lefebvre, E.Bourgeat-Lami, SiOH-Functionalized Polystyrene Latexes. A Step toward the Synthesis of Hollow Silica Nanoparticles,Chem. Mater.,14(3) (2002)1325-1331, http://dx.doi.org/10.1021/cm0112441.

[20] J.P.Matinlinna, L.V.J.Lassila, P.K. Vallittu, The effect of three silane coupling agents and their blends with a cross-linker silane on bonding a bis-GMA resin to silicatized titanium (a novel silane system), J. Dent., 34(10) (2006) 740 – 746, http://dx.doi.org/10.1016/j.jdent.2006.01.008.

[21] C.Y.K.Lung, J.P.Matinlinna, Aspects of silane coupling agents and surface conditioning in dentistry: An overview, Dent. Mater., 28(5) (2012) 467–477, http://dx.doi.org/10.1016/j.dental.2012.02.009.

[22] P.Eisenberg, R.Erra-Balsells, Y.Ishikawa, J.C. Lucas, H.Nonami, R.J.J.Williams. Silsesquioxanes Derived from the Bulk Polycondensation of [3-(Methacryloxy)propyl] trimethoxysilane with Concentrated Formic Acid: Evolution of Molar Mass Distributions and Fraction of Intramolecular Cycles, Macromolecules, 35(4) (2002) 1160-1174, http://dx.doi.org/10.1021/ma011305g.

[23] S.Altmann., J.Pfeiffer, The Hydrolysis/Condensation Behaviour of Methacryloyloxyalkyl functional Alkoxy silanes: Structure-Reactivity Relations, Monatsh. Chem., 134(8) (2003) 1081–1092, http://dx.doi.org/10.1007/s00706-003-0615-y.

[24] M.C.B.Salon, P.A.Bayle, M.Abdelmouleh, S.Boufic, M.N.Belgacem, Kinetics of hydrolysis and self condensation reactions of silanes by NMR spectroscopy, Colloids Surf., A, 312 (2008) 83–91, http://dx.doi.org/10.1016/j.colsurfa.2007.06.028.

[25] B.Riegel, S.Blittersdorf, W.Kiefer, S.Hofacker, M.Muller, G.Schottner, Kinetic investigations of hydrolysis and condensation of the glycidoxypropyltrimethoxysilane/aminopropyltriethoxy-silane system by means of FT-Raman spectroscopy I, J. Non-Cryst. Solids, 226(1-2) (1998) 76–84, http://dx.doi.org/10.1016/S0022-3093(97)00487-0.

[26] M.Guan, W.Liu, Y.Shao, H.Huang, H.Zhang, Preparation, characterization and adsorption properties studies of 3-(methacryloyloxy)propyltrimethoxysilane modified and polymerized sol–gel mesoporous SBA-15 silica molecular sieves, Micropor. Mesopor. Mat., 123(1-3) (2009) 193–201, http://dx.doi.org/10.1016/j.micromeso.2009.04.001.

[27] L.Wei, N.Hu, Y.Zhang, Synthesis of Polymer—Mesoporous Silica Nanocomposites, Materials, 3(7) (2010) 4066-4079 http://dx.doi.org/10.3390/ma3074066 .

[28] X.Ji, J.E.Hampsey, Q.Hu, J.He, Z.Yang, Y.Lu, Mesoporous Silica-Reinforced Polymer Nanocomposites Chem. Mater., 15(19) (2003) 3656-3662, http://dx.doi.org/10.1021/cm0300866.

[29] X.Cui , S.Zhong, J.Yana, C.Wanga, H.Zhanga, H.Wang, Synthesis and characterization of core–shell SiO_2-fluorinated polyacrylate nanocomposite latex particles containing fluorine in the shell, Colloids Surf. A, 360 (1-3) (2010) 41–46, http://dx.doi.org/10.1016/j.colsurfa.2010.02.006.

[30] S .Kango, S .Kalia, A.Celli, J.Njuguna, Y.Habibi, R.Kumar, Surface modification of inorganic nanoparticles for development of organic–inorganic nanocomposites, Prog. Polym. Sci. 38(8) (2013) 1232–1261, http://dx.doi.org/10.1016/j.progpolymsci.2013.02.003.

[31] K.Ishizu, Y.Tokuno, D.H.Lee, S.Uchida, M.Ozawa, Synthesis of silica hybrid nanoparticles modified with photofunctional polymers and construction of colloidal crystals, J. Appl. Pol. Sci, 112(4) (2009) 2434-2440, http://dx.doi.org/10.1002/app.29815.

[32] J.-G.Tang, Y.Wang, J.-X.Liu, S.-X.Cao, L.-J.Huang, Z.Huang, H.-L.Cong, S.-Q.Xie, Y.Wang, Adjustable Fluorescent Material of Terbium Hybrid in Poly (Methyl Methacrylate)—SiO_2 Copolymer Host, Integr. Ferroelectr., 138 (1) (2012), 138, 83-93, http://dx.doi.org/10.1080/10584587.2012.688470.

[33] E.Bourgeat-Lami, I.Tissot, F.Lefebvre, Synthesis and Characterization of SiOH-Functionalized Polymer Latexes Using Methacryloxy Propyl Trimethoxysilane in Emulsion Polymerization, Macromolecules, 35(16) (2002) 6185-6191, http://dx.doi.org/10.1021/ma012230j.

[34] H.Huang, L.He, K.Huang, M.Gao, Synthesis and comparison of two poly (methyl methacrylate-b-3-(trimethoxysilyl)propyl methacrylate)/SiO_2 hybrids by ‘‘grafting-to’’ approach, J. Colloid Interface Sci., 433 (2014) 133–140, http://dx.doi.org/10.1016/j.jcis.2014.07.027.

[35] J.J.Chung, J.R.Jones, T.K.Georgiou, Toward Hybrid Materials: Group Transfer *Polymerization* of 3-(Trimethoxysilyl)propyl Methacrylate, Macromol. Rapid Commun, 36(20) (2015) 1806−1809, http://dx.doi.org/10.1002/marc.201500356.

[36] J.J.Chung, J.R.Jones, T.K.Georgiou, Toward Hybrid Materials: Group Transfer Polymerization of 3-(Trimethoxysilyl)propyl Methacrylate, Macromol. Rapid Commun, 36(20) (2015) 1806−1809, http://dx.doi.org/10.1002/marc.201500356.

[37] B.Simionescu, M.Olaru, M.Aflori, E.C.Buruiana, C.Cotofana, Silsesquioxane-based Hybrid Nanocomposites of Polymethacrylate Type with Self-assembling Properties, Solid State Phenom., 151 (2009) 17-23 http://dx.doi.org/10.4028/www.scientific.net/SSP.151.17

[38] H.Wei, C.Cheng, C.Chang, W.Q.Chen, S.X.Cheng, X.Z.Zhang, R.X.Zhuo, Synthesis and Applications of Shell Cross-Linked Thermoresponsive Hybrid Micelles Based on Poly(N-isopropylacrylamide-co-3-(trimethoxysilyl)propyl methacrylate)-*b*-poly(methyl methacrylate), Langmuir, 24(9) (2008) 4564-4570, http://dx.doi.org/10.1021/la703320h.

[39] J.Du, Y.Chen, Atom-Transfer Radical Polymerization of a Reactive Monomer: 3-(Trimethoxysilyl)propyl Methacrylate, Macromolecules, 37(17) (2004) 6322-6328, http://dx.doi.org/10.1021/ma0359382 .

[40] J.F.Lopez, G.J.Pelaez, L.D.Perez, Monitoring the formation of polystyrene/silica nanocomposites from vinyl triethoxysilane containing copolymers, Colloid Polym. Sci., 291(5) (2013) 1143-1153, http://dx.doi.org/10.1007/s00396-012-2842-4 .

[41] K.F.Ni, G.R.Shan, Z.X.Weng, N.Sheibat-Othman, G.Fevotte, F.Lefebvre, E.Bourgeat-Lami, Synthesis of Hybrid Core-Shell Nanoparticles by Emulsion (Co)polymerization of Styrene and γ-methacryloxypropyltrimethoxysilane, Macromolecules, 38(17) (2005) 7321-7329, http://dx.doi.org/10.1021/ma050334e

[42] W.Liao, J.Qu, Z.Li, H.Chen, Preparation of Organic/Inorganic Hybrid Polymer Emulsions with High Silicon Content and Sol-gel-derived Thin Films, Chin. J. Chem. Eng., 18(1) (2010) 156-163, http://dx.doi.org/10.1016/S1004-9541(08)60337-7.

[43] P.Xu, H.Wang, R.Tong, Q.Du, W.Zhong, Preparation and morphology of SiO_2/PMMA nanohybrids by microemulsion polymerization, Colloid Polym. Sci., 284(7) (2006) 755–762, http://dx.doi.org/10.1007/s00396-005-1428-9

[44] H.H.Wang, X.R.Li, G.Q.Fei, J.Mou, Synthesis, morphology and rheology of core-shell silicone acrylic emulsion stabilized with polymerisable surfactant, Express Polym Lett, 4(11) (2010) 670–680, http://dx.doi.org/10.3144/expresspolymlett.2010.82.

[45] H.Wei, C.Cheng, C.Chang, W.Q.Chen, S.X.Cheng, X.Z.Zhang, R.X.Zhuo, Synthesis and Applications of Shell Cross-Linked Thermoresponsive Hybrid Micelles Based in Poly(N-isopropylacrylamide-co-3-(trimethoxysilyl)propyl methacrylate)-*b*-poly(methyl methacrylate), Langmuir, 24(9) (2008) 4564-4570, http://dx.doi.org/10.1021/la703320h.

[46] J.Du, Y.Chen. Atom-Transfer Radical Polymerization of a Reactive Monomer: 3-(Trimethoxysilyl)propyl Methacrylate, Macromolecules, 37(17) (2004) 6322-6328, http://dx.doi.org/10.1021/ma0359382.

[47] A.Zaichenko, O.Shevchuk, V.Samaryk, S.Voronov, The peculiarities of homogeneous nucleation of reactive Cu^0 colloidal particles in the presence of functional oligoperoxides, J. Coll. Int. Sci, 275(1) (2004) 204-213, http://dx.doi.org/10.1016/j.jcis.2004.01.074.

[48] A.Zaichenko, I.Bolshakova, N.Mitina, O.Shevchuk, A.Bily, V.Lobaz, The synthesis and rheological characteristics of colloidal systems containing functional magnetic nanoparticles, J. Magn. Mate, 289 (2005) 17-20, http://dx.doi.org/10.1016/j.jmmm.2004.11.006.

[49] V.Novikov, A.Zaichenko, N.Mitina, O.Shevchuk, K.Raevska, V.Lobaz., V.Lubenets, Yu.Lastukhin, Inorganic, Polymeric and Hybrid Colloidal Carriers with Multi-Layer Reactive Shell, Macromol.Symp., 210(1) (2004) 193 – 202, http://dx.doi.org/10.1002/masy.200450622

[50] Yu.Kit, R.Bilyy, R.Stoika, N.Mitina, A.Zaichenko, in: S.A.Kumar, S.Thiagarajan, S.-F.Wang (Eds.) Biocompatible Nanomaterials: Synthesis, Characterization and Applications, Nova Science Publishers Inc., New York, 2010, p. 209-223.

[51] V.Vistovskyy, N.Mitina, A.Shapoval, T.Malyy, A.Gektin, T.Konstantinova, A. Voloshinovskii, A Zaichenko, Luminescence properties of $LaPO_4$–Eu nanoparticles synthesized in the presence of surface active oligoperoxide as template, Opt. Mater., 34(12) (2012) 2066-2070, http://dx.doi.org/10.1016/j.optmat.2012.04.010.

[52] A.Zaichenko, N.Mitina, M.Kovbuz, I.Artym, S.Voronov, Low-temperature surface-active complex-radical oligodert.Alkylperoxidic initiators, Macromol. Symp., 164(1) (2001) 47-71, http://dx.doi.org/10.1002/1521-3900(200102)164:1<47::AID-MASY47>3.0.CO;2-F .

[53] V.R.Gowariker, N.V.Viswanathan, J.Sreedhar, Polymer Science, New Age International Ltd., New Delhi, 1986, p.505.

[54] K.Lohbeck, H.Haferkorn, W.Fuhrmann, N.Fedtke. Maleic and Fumaric Acids, Ullmann's Encyclopedia of Industrial Chemistry, Vol.20, Wiley-VCH Verlag GmbH &Co.KGaA, New York 2002;. http://dx.doi.org/10.1002/14356007.a16_053

[55] S.A.Voronov, E.M.Kiselyov, S.S.Minko, O.G.Budishevska, Y.V.Roiter, Structure and reactivity of peroxide monomers, J. Polym. Sci. Pol. Chem. 34(12) (1996) 2507–2511, http://dx.doi.org/10.1002/(SICI)1099-0518(19960915)34:12<2507::AID-POLA24>3.0.CO;2-B.

[56] A.Zaichenko, N.Mitina, M.Kovbuz, I.Artym, S.Voronov, Surface-active metal-coordinated oligoperoxidic radical initiators. I. The interrelation between the microstructure of ditertiary oligoperoxides and their ability to form stable metal complexes, J. Pol. Sci., 38(3) (2000) 516-527, http://dx.doi.org/10.1002/(SICI)1099-0518(20000201)38:3<516::AID-POLA18>3.0.CO;2-R.

[57] A.Zaichenko, S.Voronov, A.Kuzaev, O.Shevchuk,V.Vasiliev, Control of microstructure and molecular weight distribution of carbon-chain heterofunctional oligoperoxidic curing agents, J.Appl.Pol. Sci., 70(12) (1998) 2449-2455, http://dx.doi.org/10.1002/(SICI)1097-4628(19981219)70:12<2449::AID-APP17>3.0.CO;2-D.

[58] M.Stickler, Experimental techniques in free radical polymerization kinetics, Macromol. Symp, 10-11(1) (1987) 17-69, http://dx.doi.org/10.1002/masy.19870100104.

[59] G.Odian, Principles of Polymerization, Fourth Edition; John Wiley &Sons: Hoboken, New Jersey, 2004, P.812.

[60] G.Schimmel, Elektronen mikroskopische methodik, Springer-Verlag, Berlin-NewYork,1969, p.244.

[61] B.A.Zasońska, N.Boiko, D.Horák, O.Klyuchivska, H.Macková, M.J.Benes, M.Babic, M.Trchová, J.Hromádková, R.Stoika, The Use of Hydrophilic Poly(N,N-dimethylacrylamide) for Promoting Engulfment of Magnetic γ-Fe_2O_3 Nanoparticles by Mammalian Cells, J. Biomed. Nanotechnol., 9(3) (2013) 479–491, https://doi.org/10.1166/jbn.2013.1552.

[62] A.S.Zaichenko, S.A.Voronov, N.E.Mitina, Low temperature initiating by di-*tert*-alkyl peroxides of the water dispersion polymerization of styrene, Reports of the National Academy of Sciences of Ukraine (in Ukrainian), 9 (1998) 152-157.

[63] P.D.Bartlett, H.Kwart, Some Inhibitors and Retarders in the Polymerization of Liquid Vinyl Acetate. II. 1,3,5-Trinitrobenzene and Sulfur. J.Am.Chem.Soc. 74(16) (1952) 3969–3973, https://doi.org/10.1021/ja01136a001

Highlights:

- Luminescent polymer-SIO2 nanoparticles (NPs) were synthesized via polymerization of trimethoxysilane propyl methacrylate (MPTS) initiated by oligoperoxide (OMC).
- Contribution of the reactions of MPTS reactive centers depends on OMC concentration.
- The OMC concentration defines kinetics of the formation and morphology of the NPs.
- Luminescent NPs were tolerated and well attached to murine leukemia L1210 cells.